CENTER FOR TRANSPORTATION INFRASTRUCTURE AND SAFETY

Extending the Usage of High Volume Fly Ash in Concrete

by

Jeffery S. Volz, SE, PE, PhD (Principal Investigator)
Tyler Ley, PE, PhD (Co-Principal Investigator)
Jonathan Drury
Qinang Hu
Morteza Khatibmasjedi
Corey Wirkman

A National University Transportation Center at Missouri University of Science and Technology

Disclaimer

Technical Report Documentation Page

1. Report No.	2. Government Accession No.	3. Recipient's Catalog No.
NUTC R336		

4. Title and Subtitle	5. Report Date
Extending the Usage of High Volume Fly Ash in Concrete	July 2014
	6. Performing Organization Code
7. Author/s Jeffery S. Volz, SE, PE, PhD (Principal Investigator) Tyler Ley, PE, PhD (Co-Principal Investigator) Jonathan Drury Qinang Hu Morteza Khatibmasjedi Corey Wirkman	8. Performing Organization Report No. Project # 00042492
9. Performing Organization Name and Address Center for Transportation Infrastructure and Safety/NUTC program Missouri University of Science and Technology 220 Engineering Research Lab Rolla, MO 65409	10. Work Unit No. (TRAIS) 11. Contract or Grant No. DTRT06-G-0014
12. Sponsoring Organization Name and Address U.S. Department of Transportation Research and Innovative Technology Administration 1200 New Jersey Avenue, SE Washington, DC 20590	13. Type of Report and Period Covered Final 14. Sponsoring Agency Code

15. Supplementary Notes

16. Abstract

Concrete is the world's most consumed man-made material. Unfortunately, the production of Portland cement, the active ingredient in concrete, generates a significant amount of carbon dioxide. For each pound of cement produced, approximately one pound of carbon dioxide is released into the atmosphere. With cement production reaching nearly 6 billion tons per year worldwide, the sustainability of concrete is a very real concern.

Since the 1930's, fly ash – a pozzolanic material – has been used as a partial replacement of Portland cement in concrete to improve the material's strength and durability, while also limiting the amount of early heat generation. From an environmental perspective, replacing cement with fly ash reduces concrete's overall carbon footprint and diverts an industrial by-product from the solid waste stream (currently, about 40 percent of fly ash is reclaimed for beneficial reuse and 60 percent is disposed of in landfills).

Traditional specifications limit the amount of fly ash to 25 or 30 percent cement replacement. Recent studies, including those by the investigators, have shown that higher cement replacement percentages – even up to 75 percent – can result in excellent concrete in terms of both strength and durability. Referred to as high-volume fly ash (HVFA) concrete, this material offers a viable alternative to traditional Portland cement concrete and is significantly more sustainable. By nearly doubling the use of reclaimed fly ash in concrete, HVFA concrete aligns well green initiatives on recycling. However, HVFA concrete is not without its problems. At high replacement rates, HVFA concrete has shown very poor scaling resistance and mixed results with regard to other durability measures.

The objective of this research was to determine the implications of increasing the amount of fly ash in concrete with regard to durability. This report consists of two parts. Part I investigates the mechanism of salt scaling in HVFA concrete, while Part II investigates the full range of durability resistance including freeze-thaw, chloride permeability, and scaling. The results indicate that fly ash replacement levels up to 50% result in concrete that possesses excellent durability.

17. Key Words	18. Distribution Statement
Cement, Concrete, Durability, Fly Ash, Mix Design, Sustainability.	No restrictions. This document is available to the public through the National Technical Information Service, Springfield, Virginia 22161.

19. Security Classification (of this report)	20. Security Classification (of this page)	21. No. Of Pages	22. Price
unclassified	unclassified	42	

Form DOT F 1700.7 (8-72)

FINAL Report

Extending the Usage of High Volume Fly Ash in Concrete

By

Jeffery S. Volz, SE, PE, PhD (Principal Investigator)
Tyler Ley, PE, PhD (Co-Principal Investigator)
Jonathan Drury
Qinang Hu
Morteza Khatibmasjedi
Corey Wirkman

May 2014

Part I: Insights into the Mechanisms of Salt Scaling of High Volume Fly Ash Concrete

Final Report: May 2014

Morteza Khatibmasjedi
Qinang Hu
Tyler Ley, Ph.D., P.E.

Oklahoma State University
Civil and Environmental Engineering Department
207 Engineering South
Stillwater, OK 74078

Introduction

It is widely recognized that high volume fly ash (HVFA) concrete is capable of producing concrete with satisfactory strength and long term durability in a number of environments. One major issue with the widespread usage of concrete with high volume fly ash is that the resulting concrete is not durable from salt scaling during freezing. The seminal work on this topic was done by D. Whiting (1989). Based on a limited number of tests it was observed that as the fly ash content in a mixture increased, then so did the amount of salt scaling that occurs. Because of this publication, many codes have limited the amount of fly ash to 25% for concrete elements with a large surface to volume ratio. This usually impacts concrete that is exposed to deicing salts, such as pavements, bridge decks, and sidewalks.

While several other papers have been published that have shown similar findings, only limited work has been done to investigate the mechanisms of this deterioration. This work aims to better understand the mechanisms of salt scaling from freezing in general with a special focus on mixtures with high volumes of fly ash. This work was done by combining large scale tests with concrete (ASTM C 672) and mortar sieved from the concrete mixtures. This mortar was also used in small scale experiments where X-ray micro computed tomography (mCT) was used to study the initiation and propagation of damage in the microstructure from the salt scaling caused by freezing. Although more work is needed before strong conclusions can be drawn, this work provides some useful insights from the experimental work not previously published.

Experimental Methods

Materials

A Type I cement meeting the requirements of ASTM C150 and Type C fly ash according to ASTM C618 was used in this study. Table 1 shows the oxide analysis from X-ray Fluorescence (XRF). Locally available crushed limestone with a nominal maximum aggregate size of 1” was used as course aggregate and natural sand as the fine aggregate.

Table 1 - The oxide analysis of cement and fly ash 1 and fly ash 2.

Oxide	Chemical Test Results (%)		
	Cement	Fly Ash 1	Fly Ash 2
SiO_2	20.77	38.71	33.44
Al_2O_3	4.57	18.82	18.6
MgO	2.37	5.55	5.2
Fe_2O_3	2.62	5.88	7.26
CaO	62.27	23.12	25.2
SO_3	3.18	1.27	4.27
Na_2O	0.19	1.78	1.76
K_2O	0.32	0.58	0.48
TiO_2	0.34	1.35	1.49
P_2O_5	0.14	1.46	1.47
SrO	0.22	0.39	0.42
BaO	0.07	0.72	0.84
MnO_2	-	0.02	0.03

Mixture design

In this study five concrete mixtures were used with water to cementitious material ratio (w/cm) of 0.45. Two mixtures with just Portland cement were investigated. One had no air entraining agent (AEA) and the other uses AEA to stabilize approximately 6% air. Two mixtures used a 50% replacement of cement with fly ash by mass, and one used a 70% mass replacement. All of these mixtures used AEA to stabilize approximately 6% air in the mixture. Table 2 shows the SSD mixture design proportions.

Mixing Procedure

Aggregates were collected from outside storage piles and brought into the mixing room where they were thoroughly mixed and samples were taken for moisture correction. These samples were oven dried to obtain the moisture content of aggregates and the weights of each material was adjusted based on moisture condition. At the time of mixing, all aggregates were loaded into the mixer along with approximately one-third of the mixing water. This combination was mixed for three minutes to ensure that the aggregates were evenly distributed. Next, the cementitious materials and the remaining water were added and mixed for three minutes. The resulting mixture rested for two minutes while the sides of the mixing drum were scraped. After the rest period, the mixer was turned on and AEA was added (if applicable). After the addition of AEA the concrete was mixed for three minutes.

Table 2 - The SSD Mixture Proportions used in this study.

Mixture	Cement ($lb./yd^3$)	Fly Ash		Coarse Aggregate ($lb./yd^3$)	Fine Aggregate ($lb./yd^3$)	Water ($lb./yd^3$)	w/c
		Amount ($lb./yd^3$)	Type				
Non Air Entrained100 % Cement	611	0	-	1850	1203	275	0.45
Air Entrained 100% Cement	611	0	-	1850	1203	275	0.45
Air Entrained 50% Fly Ash 1	305.5	305.50	1	1820	1190	275	0.45
Air Entrained 50% Fly Ash 2	305.5	305.50	2	1820	1190	275	0.45
Air Entrained 70% Fly Ash 2	169.2	394.8	2	1720	1200	253.8	0.45

Fresh and Hardened Concrete Properties Testing

After mixing, the slump (ASTM C143) and air content (ASTM C231) were used to evaluate the fresh concrete. For each mixture three 4x8 cylinders were obtained for compressive strength testing at 28 days. Also a sample for hardened air void analysis was made. Six samples for the ASTM C672 salt scaling test were taken from each mixture. Three of these samples were filled with concrete and three with mortar obtained by removing the aggregates from the concrete. For the mortar samples the concrete was placed on a plastic mat and aggregates were removed by hand. Each container was filled, rodded, and tapped in two layers. The samples were finished with a plastic strike off board. Once the concrete was firm, the specimens were broom finished. The samples were then sealed in their containers and cured in the mixing room for 24 hours. All of this was done in accordance to ASTM C672.

In addition, two kinds of small cylinders were made for mCT investigation. Plastic cylinders with 5/16” and 3/16” diameter were cut into 0.5” sections. Each section was filled with 1/8” of mortar. The samples were consolidated by holding the plastic cylinder in one hand and clapping it into the other 30 times. A needle was used to clean the sides of the straw and finish the sample. The straws were then cured in a sealed container for 24 hours.

The samples for salt scaling and compressive strength were removed from the molds after 24 hours and placed in a moist room. At the age of 14 days, the salt scaling and mCT specimens were removed from the moist room and stored in a chamber at 74°F and 40% relative humidity for 14 days. The samples for mCT were cured the same as the larger samples. This follows the procedures of ASTM C672.

Salt scaling test

After curing, the salt scaling and mCT specimens were covered with ¼" of 4% calcium chloride solution. The specimens were then placed in a freezer for 16 to 18 hours and then removed and allowed to thaw in a 73.5 ± 3.5°F environment while sealed for about 6 to 8 hours. The specimens were placed back in the freezer after the thawing period. Each specimen was subjected to 50 freeze-thaw cycles. Every five cycles the solution was drained and the specimens were rinsed with tap water to remove any loose material and visually rated according to ASTM C672. The samples were also weighed to obtain the mass change. One challenge with the salt scaling test is that the results are subjective because they are based on visual observations. Weight change measurement has been suggested to provide quantitative data to compare the sample performance. A picture of each specimen was also taken after each five cycles for future references. It should be noted that it was not possible for the mortar samples to receive a visual ranking of 5. As described in Table 3, it is only possible to get a ranking of 5 if the coarse aggregate are visible over the entire surface. Since there are no coarse aggregates in the mixture this was not possible.

Table 3 – A summary of the ASTM C672 visual rating.

Rating	Condition
0	No scaling
1	Very slight scaling {3 mm (1/8 in.)} depth max (no coarse aggregate visible)
2	Slight to moderate scaling
3	Moderate scaling (some coarse aggregate visible)
4	Moderate to severe scaling
5	Severe scaling (coarse aggregate visible over entire surface)

Radiography and Tomography

Cylinder specimens were investigated with a SkyScan 1172 MicroCT scanner to produce radiography data in order to study the salt scaling on the micron scale. These samples were treated and conditioned the same as the larger samples. The salt solution was replaced and a radiograph of each specimen was taken at three angles every four cycles. The radiographs were used as a tool to determine if there was any major change in the samples. If a major change was observed, then a full tomograph scan was taken. If there was no change then the test was continued.

The scanning parameters used to investigate the samples are summarized in Table 4. Effort was make to keep all of the scan parameters constant over the test. However, as salt scaling and subsequent mass loss occurred, it was necessary to adjust the voltage of the instrument to keep the minimum X-rays passing through the sample in the range of 30% to 50%. A combination of Matlab and Amira was used for the image analysis and visualization.

Table 4 – A summary of the scan parameters used.

Scan Parameter	3/16" diameter	5/16" diameter
Camera Type	4k	4k
Pixel size (um)	1 - 2	2 – 4
Filter	Al +Cu	Al +Cu
Voltage (kv)	60 - 100	70 – 100
Minimum Passing (%)	30 - 50	30 – 50
Maximum Passing (%)	90 - 100	90 – 100
Vertical Position (mm)	50 - 55	50 – 55

Results

Fresh and hardened concrete properties

Slump, air content, hardened air void analysis, and compressive strength results are reported for each mixture in Table 5. Compressive strength of cylinders was measured after 28 days curing and was reported as the average strength of three cylinders. Fresh and hardened concrete property results are shown in Table 5.

Table 5 - Fresh and hardened concrete properties.

Mixture	Slump (in.)	Air content (%)	Spacing Factor (in)	Specific Surface (in^{-1})	Void Frequency (in^{-1})	28-Day Compressive Strength (psi)
100% Cement	2.25	0.7	-	-	-	6267
100% Cement	3.5	6.9	0.0053	756.6	9.98	4741
50% Fly Ash 1	9.5	7.3	0.0052	751.8	8.35	4353
50% Fly Ash 2	7.5	10.45	0.0039	694.8	19.57	3359
70% Fly Ash 2	8	8.2	-	-	-	2581

As seen in table 5 the 28 day compressive strength was observed to decrease as the fly ash content increased. The mixtures with fly ash showed increased slump over the mixtures where none was used.

Visual Rating and Weight Loss from Salt Scaling

The average cumulative mass loss is shown in Figure 1. Concrete samples are shown by solid lines and mortar by dashed lines. Table 6 shows the average rating values and time necessary to reach that visual rating.

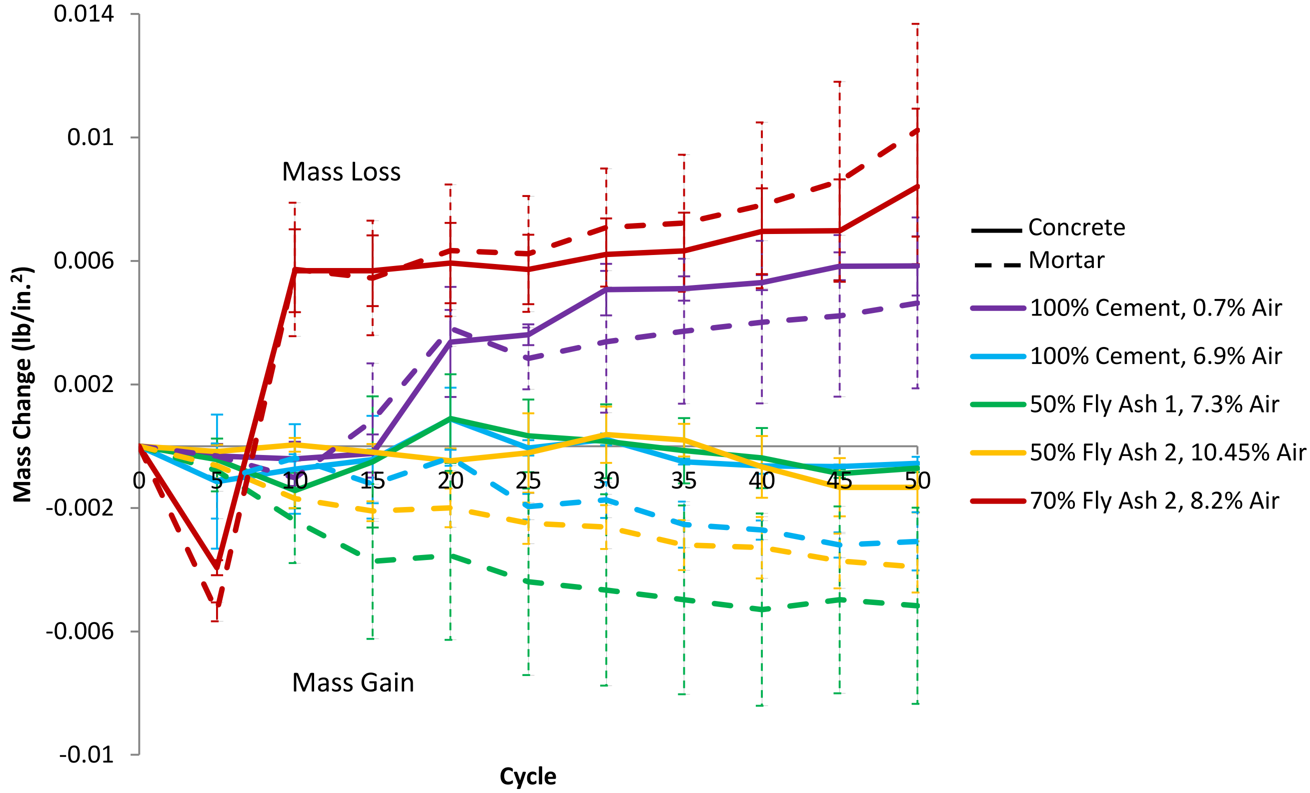

Figure 1 – Mass change for the concrete and mortar samples with freeze thaw cycles. A solid line corresponds to a concrete sample and a dashed line is a mortar sample.

Table 6 – Visual rating and mass loss for concrete and mortar salt scaling specimens.

Mixture	Air content (%)	Concrete			Mortar		
		Ultimate visual rating	Time to achieve ultimate visual rating (cycles)	Cumulative mass loss when it reaches ultimate visual rating (x 10^{-3} lb/in^2)	Ultimate visual rating	Time to achieve ultimate visual rating (cycle)	Cumulative mass loss when it reaches ultimate visual rating (x 10^{-3} lb/in^2)
100% Cement	0.7	5	30	5.06 (0.84)	3	40	4.02 (2.63)
100% Cement	6.9	2	5	-1.15 (2.17)	2	10	-0.383 (0.128)
50% Fly Ash 1	7.3	3	25	0.341 (1.18)	1	5	-0.795 (0.667)
50% Fly Ash 2	10.45	2	10	0.043 (0.213)	1	5	-0.625 (0.412)
70% Fly Ash 2	8.2	5	5	3.93 (0.241)	4	5	5.37 (0.312)

*The value in parenthesis shows one standard deviation.

Since the specimen mass was monitored during the testing it showed that the samples typically gained moisture and then subsequently lost it. This gain in moisture is hypothesized to be from the salt solution entering the sample. The loss in mass is likely from the loss of material from scaling. It is interesting to note that the samples that showed little damage continued to gain mass over the life of the test. This is likely caused by the increased saturation of the samples from the external moisture. This mass gain was more prevalent in mortar samples than concrete. This is covered further in the discussion.

2D Radiography

Results from the radiography shows that one can see changes in the samples as the damage occurs. Typical results are shown in Figures 2 through 11. The results have been arranged so that repeated images from the same orientation and at a comparable height for different freeze thaw cycles. This makes it easier to compare between the images and observe cracks and section loss that occurs.

The radiograph data and salt scaling data from the concrete and mortar were largely in agreement. Radiographs of the 70% fly ash and the non-air entrained 3/16" sample showed severe salt scaling damage. However, the non-air entrained 5/16" sample did not show major changes. This needs to be investigated in more detail. The section loss from salt scaling started after 20 cycles for most of the samples, except for the 70% fly ash 5/16" sample which begun to scale after only a few cycles. It should be noted that this sample had the worst performance in the concrete and mortar testing. There was some difference in performance between samples from the same mixtures but of different sizes. For the 50% fly ash and air-entrained 100% cement samples the 5/16" diameter samples showed more significant damage then the 3/16" samples from the same mixture. It is not clear what caused this but it does appears that there were more fine aggregate in the larger samples and this is likely important and will be further covered in the discussion.

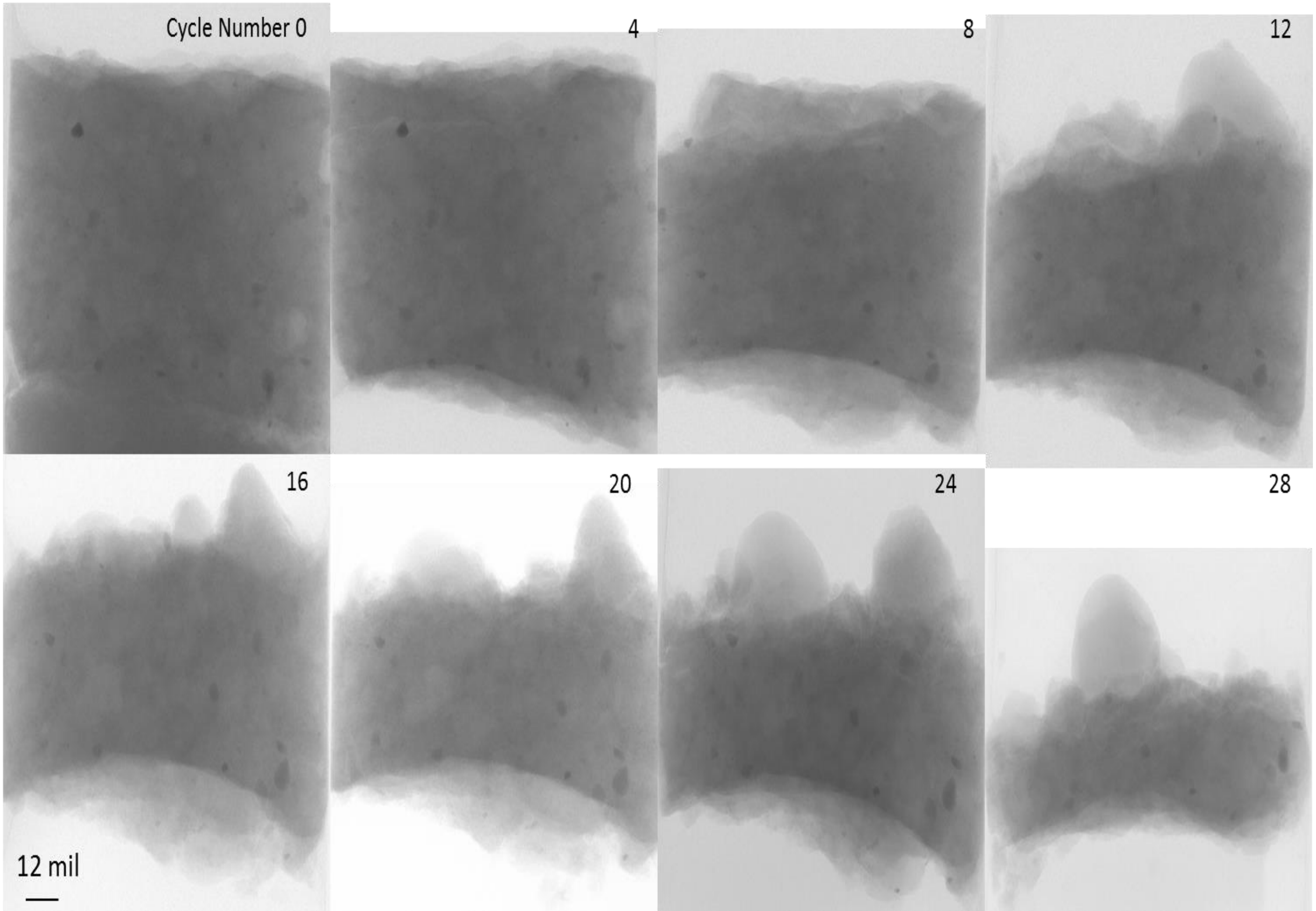

Figure 2 – A 3/16” diameter sample with 100% cement and 0.7% air content.

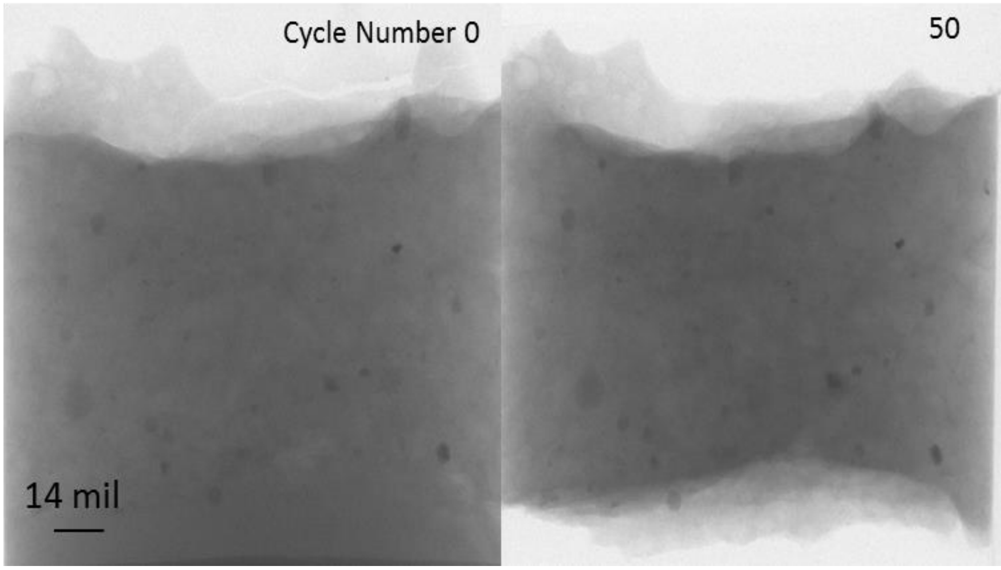

Figure 3 – A sample of 100% cement and 0.7% air from the same mixture as the one shown in Fig. 2. This sample has 5/16" diameter and the damage is much less.

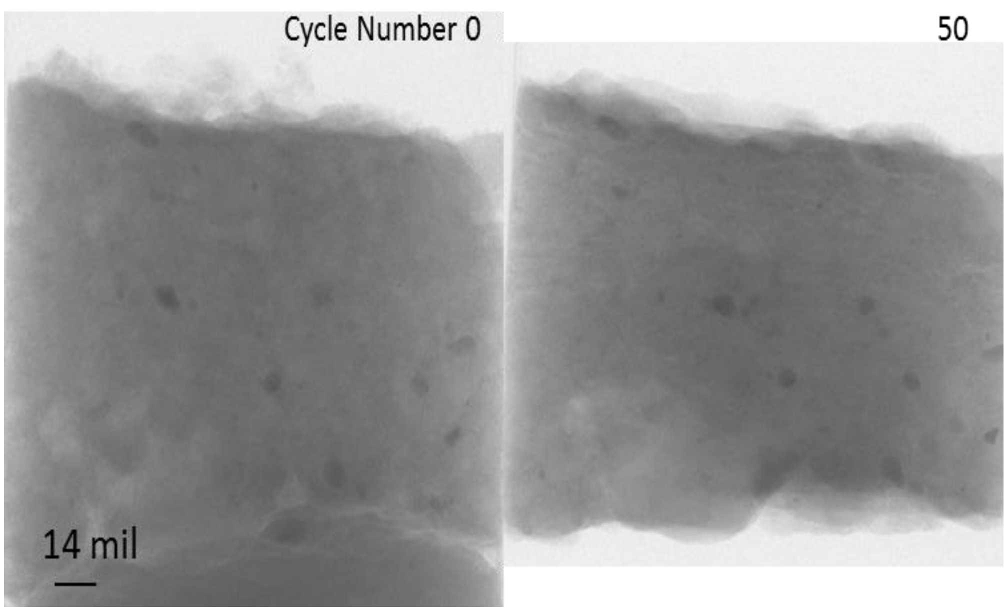

Figure 4 – A sample with 100% cement and 6.9% air content that is 3/16" in diameter showing very little damage over the 50 cycles.

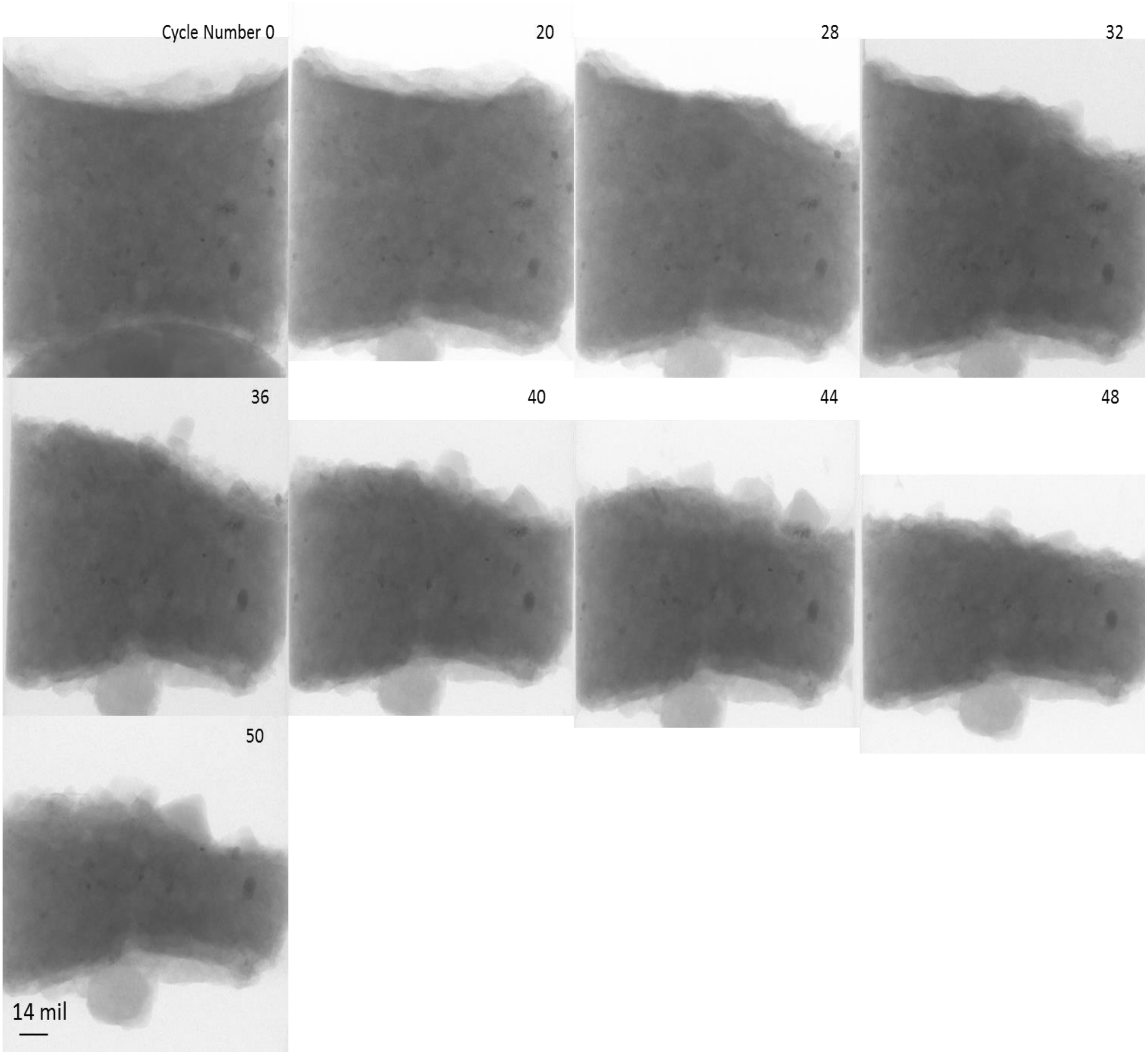

Figure 5 - A sample with 100% cement and 6.9% air content that is 5/16” in diameter showing progressive damage over the 50 cycles. This is the same sample as in Fig. 4 but it has a larger diameter.

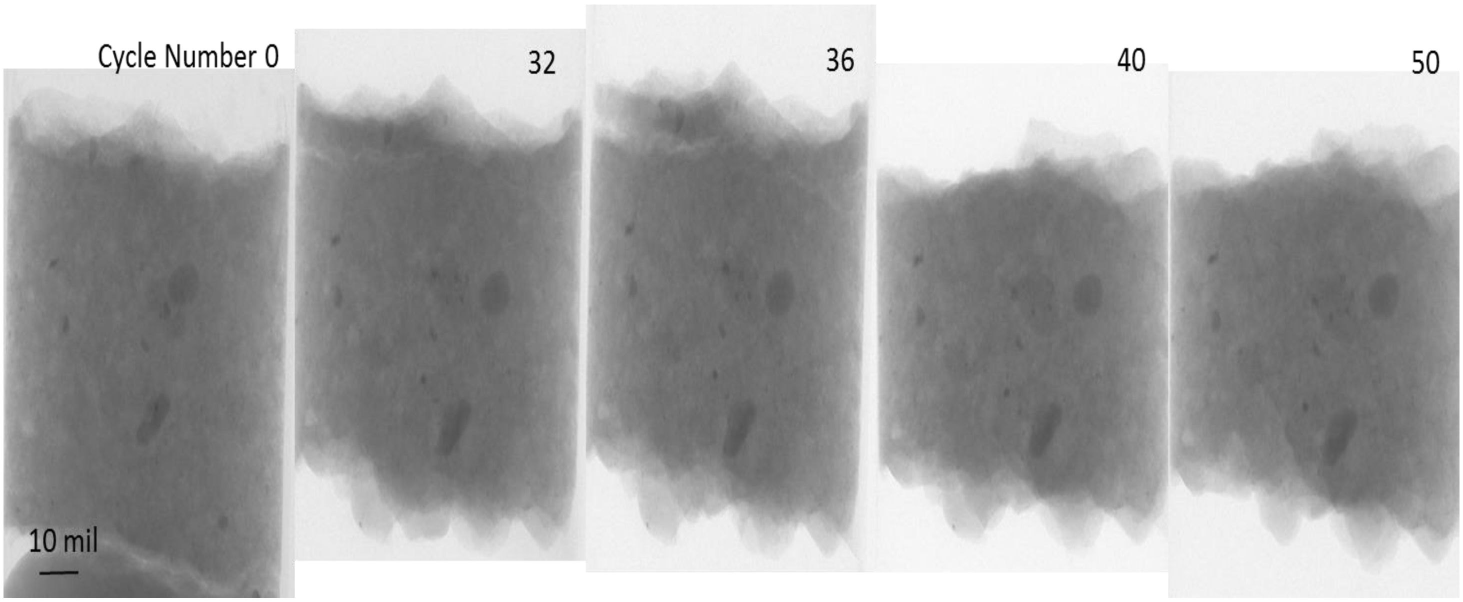

Figure 6 - A sample with 50% Fly ash 1 and 7.3% air content that is 3/16" in diameter showing limited damage over the 50 cycles.

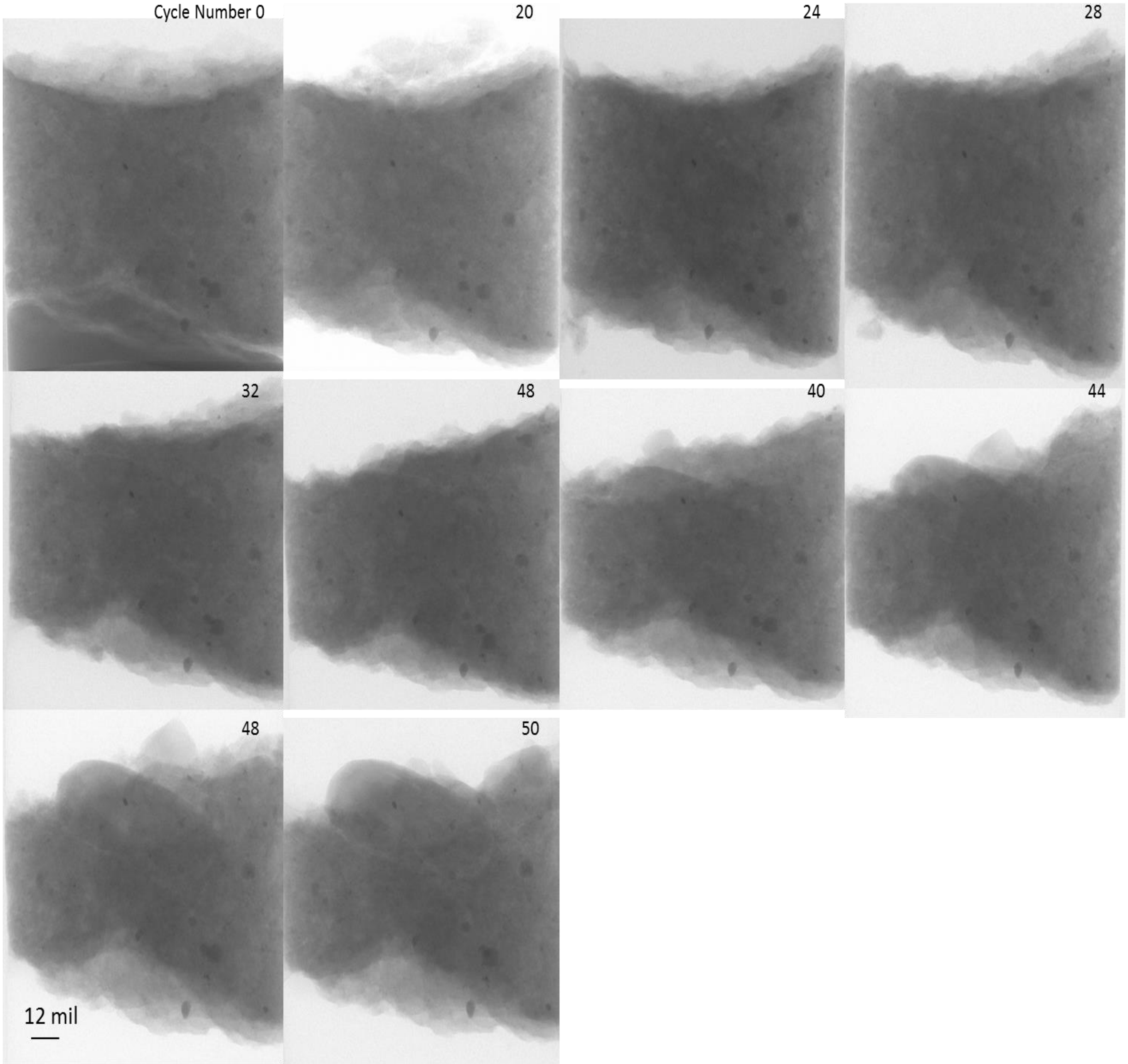

Figure 7 – A sample with 50% Fly ash 1 and 7.3% air content that is 5/16" in diameter. This is the same sample as in Fig. 6 only it has a larger diameter and is showing increased damage.

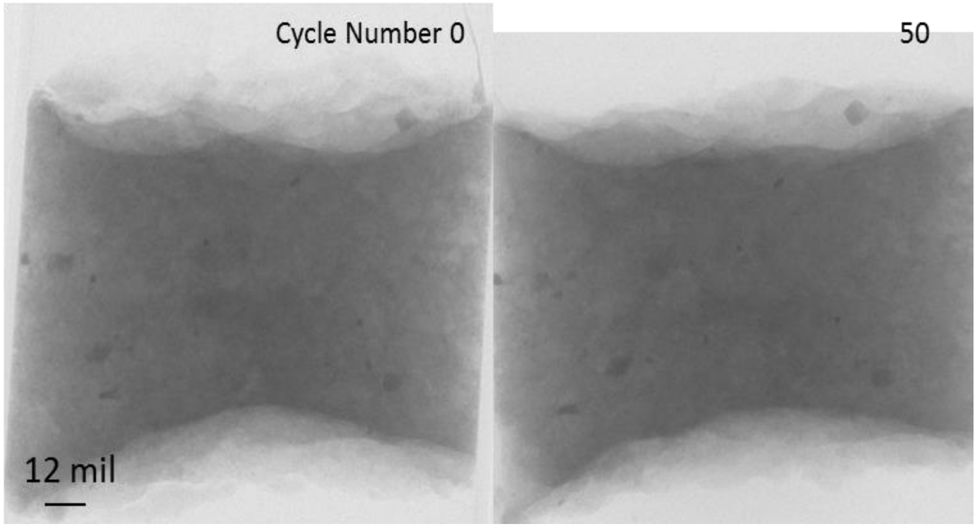

Figure 8 - A sample with 50% Fly ash 2 and 10.45% air content that is 3/16” in diameter. The sample shows very little damage over 50 cycles.

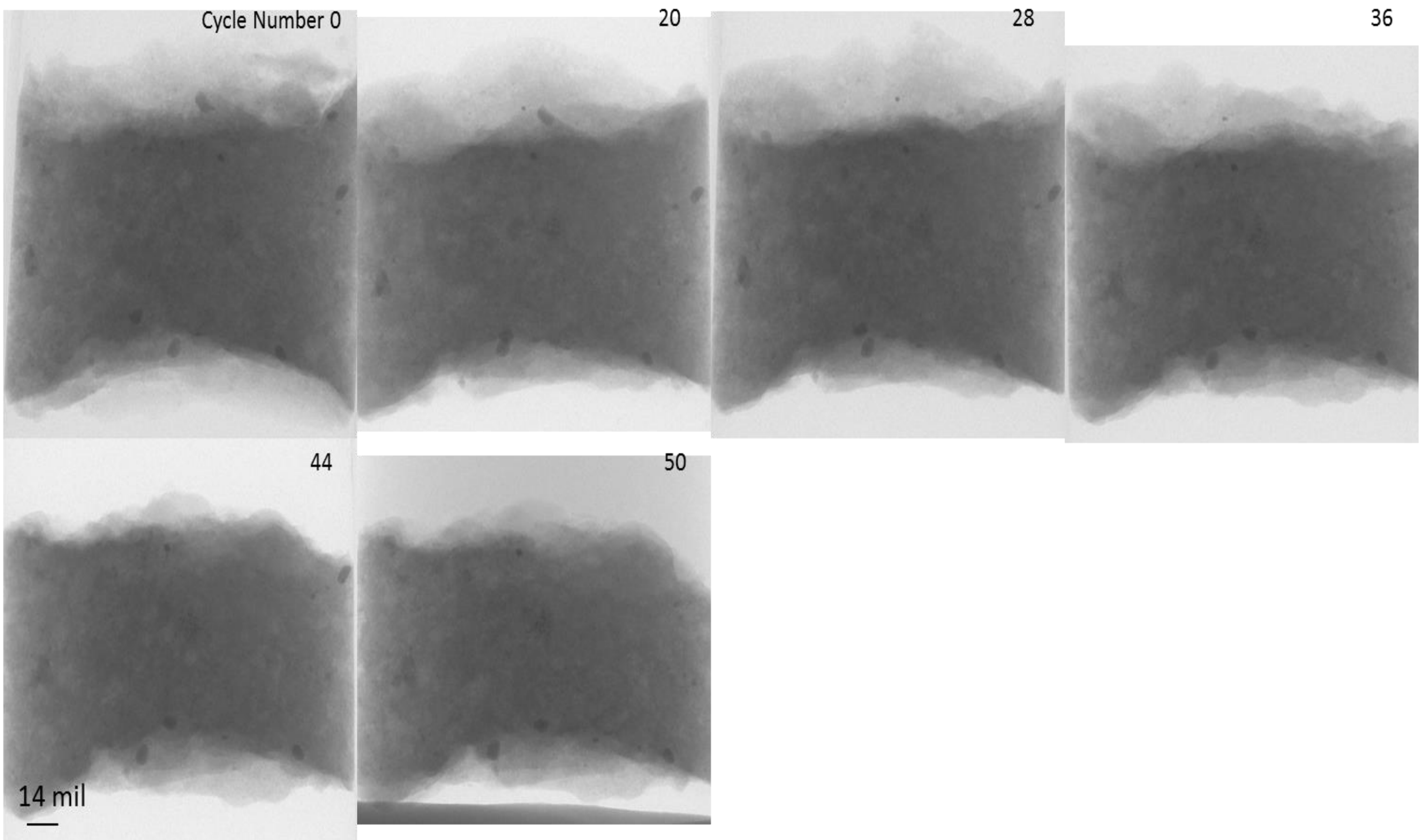

Figure 9 - A sample with 50% Fly ash 2 and 10.45% air content that is 5/16” in diameter. The sample is the same as Figure 8 and shows moderate damage over the 50 cycles.

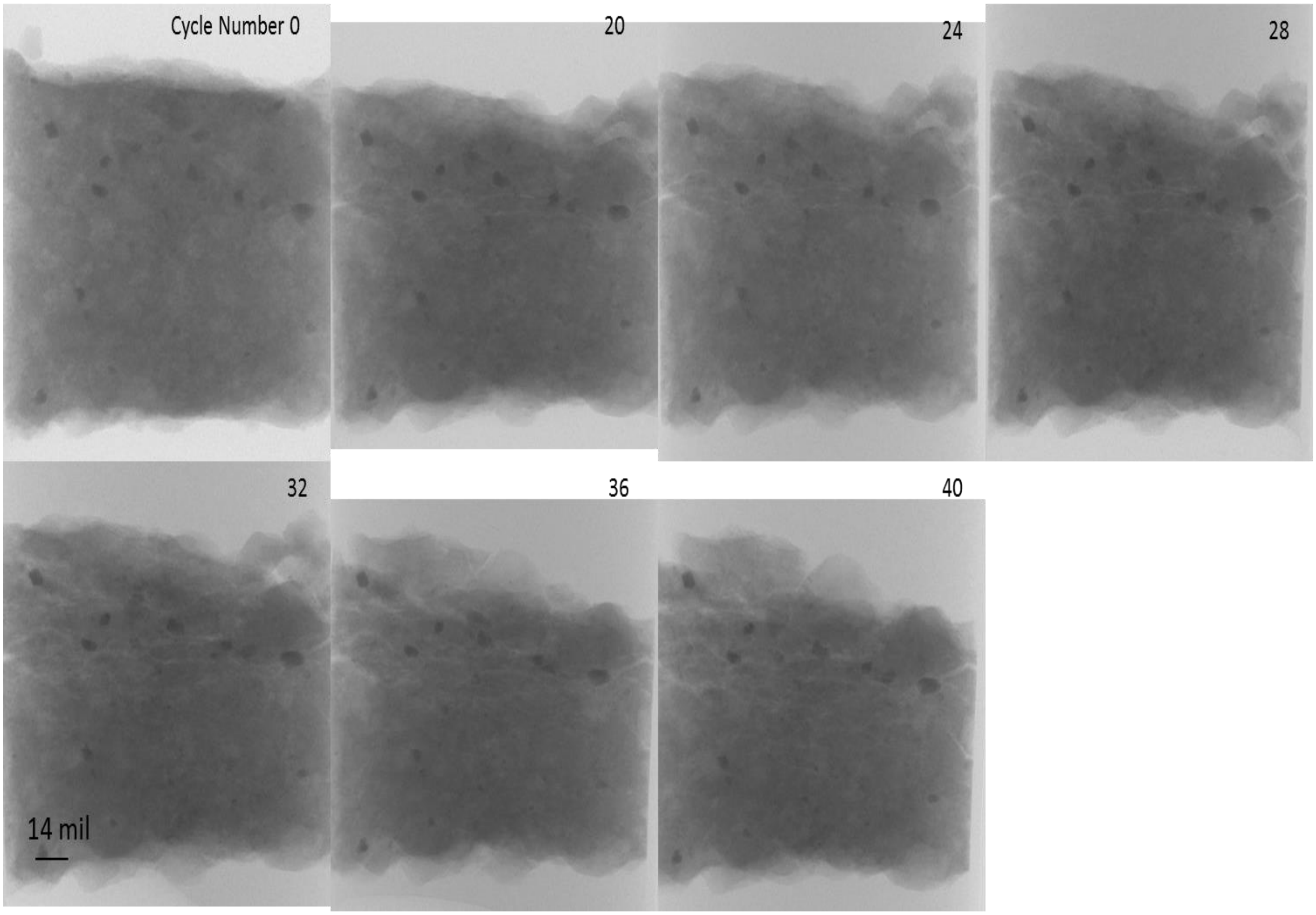

Figure 10 – A sample with 70% Fly ash 2 and 8.2% air content that is 3/16" in diameter. The sample shows a different failure mode then the other samples investigated.

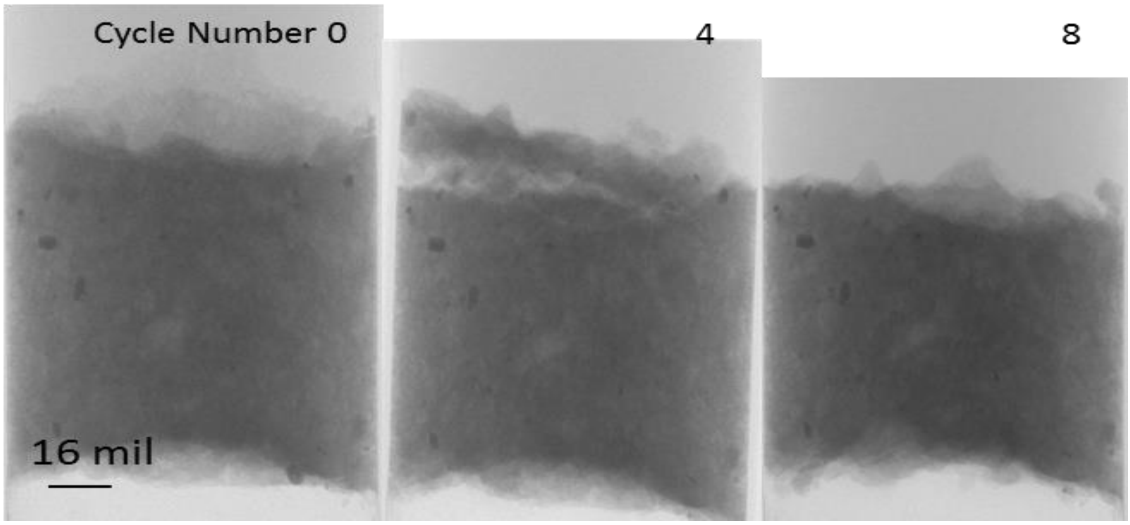

Figure 11 - A sample with 70% Fly ash 2 and 8.2% air content that is 5/16" in diameter. This is the same material as is shown in Fig. 10. Again a different failure mode is observed then the other samples investigated.

3D Tomography

A large number of tomographs were captured for this project; however, not all of them have been analyzed. A standard method to investigate the data has been established where 3D data sets are first aligned and then compared over time. A comparison is made by subtracting the two samples from one another and showing the material that is no longer part or has scaled off of the sample. An overview of the technique is shown in Figure 12. Also, the internal air void system in the sample has been shown in Figure 12 for clarity. Little was done with this information in this study, but it will be used in future analysis. A detailed analysis for the sample with 70% fly ash 2 and 8.2% air content has been completed and is given in Figure 13. In this figure the material that has left the sample between different cycles is highlighted. Also, the volume that has scaled can be estimated. In Figure 14 all of the material that has scaled from the sample is combined into a single image. A cross section is shown to highlight how the material is scaling away from the surface in layers. These measurements have the potential to make great changes in the understanding of salt scaling mechanisms. Future work will be done with the other samples to gain more insight.

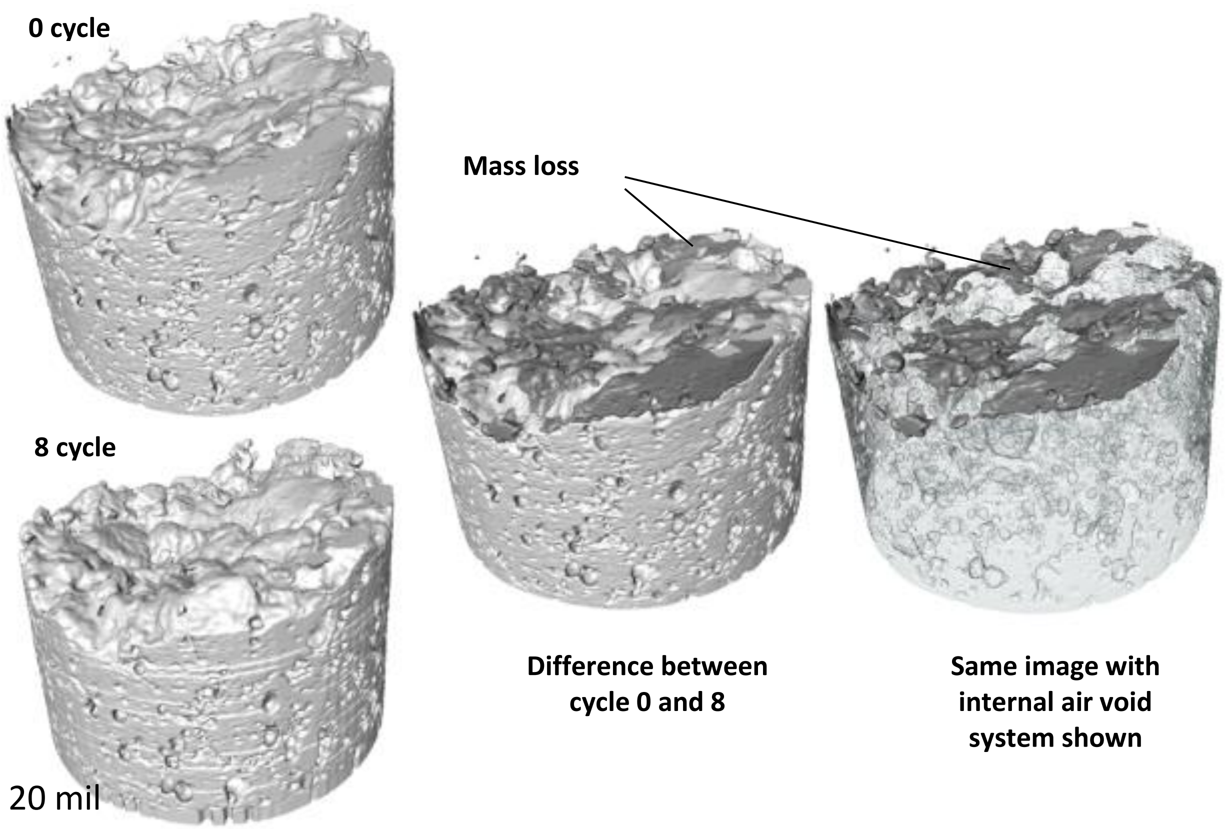

Figure 12 – An overview of the tomography analysis between two cycles. The 3D models of the sample at zero and eight freeze thaw cycles. In the middle image a 3D model is shown with the material that has scaled off the sample shown in a darker color. The image on the far right shows the same sample with the internal air void system.

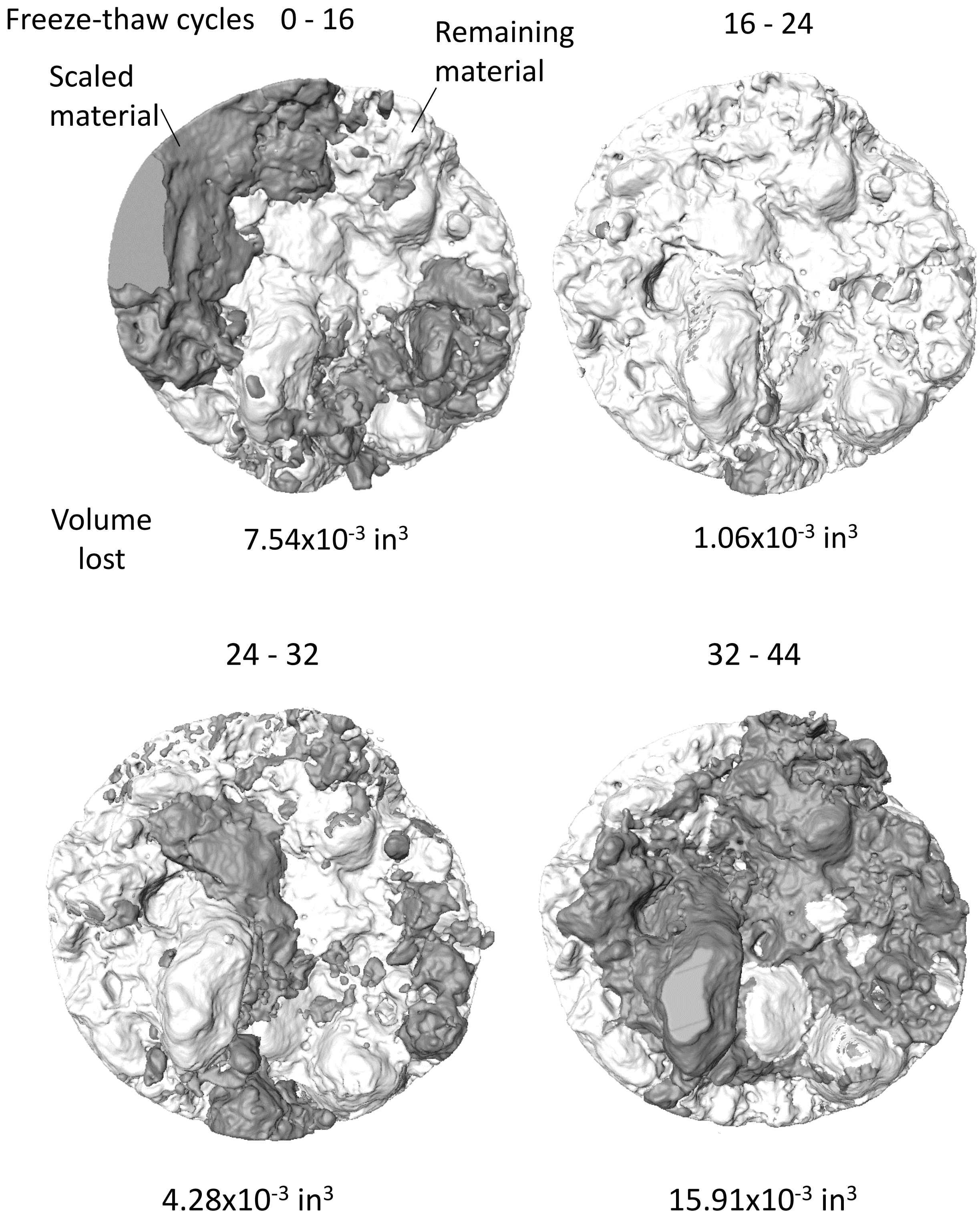

Figure 13 – 3D tomography of the top surface of the samples showing how they change over different freeze-thaw cycles. The volume loss is also shown below each of the samples.

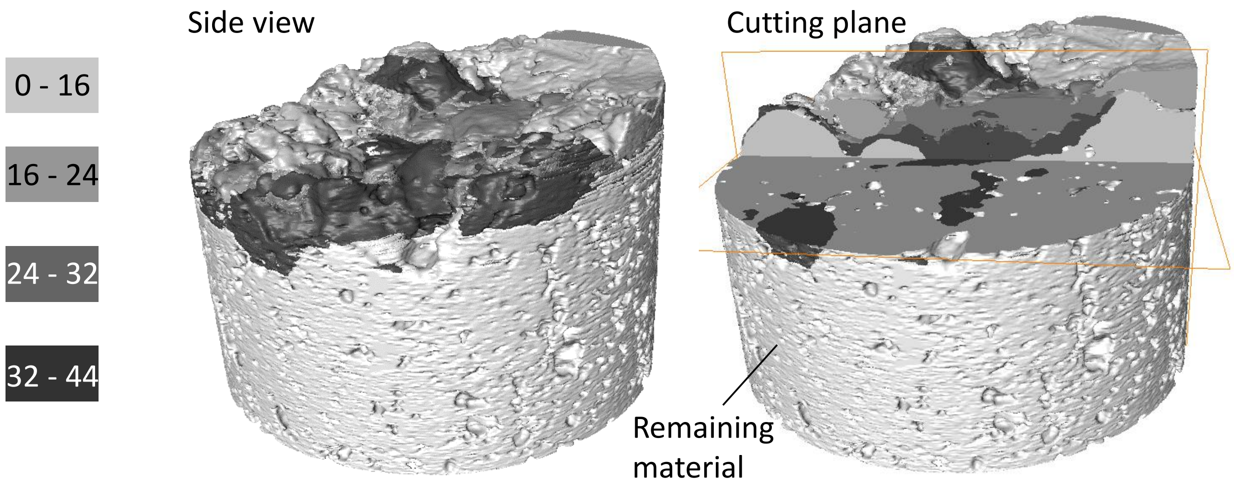

Figure 14 – This model shows the material that has left the surface of the sample in different shades of gray. A cross section is shown in the second image. It shows that the materials are leaving in layers from the outside surface of the sample.

Discussion

Properties and Salt Scaling Performance of Concrete and Mortar

The high volume fly ash mixtures showed higher workability than the mixtures with just cement; however, the 28-day compressive strength of the high volume fly ash mixtures decreased as the volume of fly ash increased. It may not be fair to compare these mixtures at only 28 days since the fly ash may contribute secondary reactions that should increase the strength over time. Also, with the increase in workability, it may be possible to decrease the water content in the mixture and therefore decrease the water to cement ratio. This should help overcome some of the strength loss of the mixtures and could be investigated with future work.

According to Table 6 and Figure 1, the mixtures that were air entrained and contained 50% fly ash or 100% cement showed great performance in the salt scaling tests. Many of these samples had a visual ranking of 2, and only one had a ranking of a 3. This data shows satisfactory freeze thaw performance for fly ash at a higher replacement rate than has been suggested in the past. While this should be investigated with a wider array of materials, the increase in fly ash replacement up to 50% will lead to great improvements in economy and sustainability and is an important contribution of this work.

The sample that was not air entrained and the sample with 70% fly ash that was air entrained did not perform well in these same tests. This confirms the recommendations by many building codes and previous publications. The results from the 70% fly ash sample is interesting because the mixture had a good air content and air void parameters from the hardened air void analysis but did not show satisfactory scaling performance. One area of interest is that the strength of the sample was much lower than the others investigated. This could be a contributor to the poor performance in the testing. This is a variable that should be isolated in future testing.

The samples in this test were specifically designed to allow them to be weighed throughout the salt scaling testing. This was done because it is challenging to isolate and measure the material that scales off of the samples. This also allowed insight into how the sample gained mass from the salt solution placed on the surface. As shown in Figure 1, every mixture gained mass during the first few cycles of testing because of water absorption. This mass gain was much larger for the 70% fly ash mixture than any other sample. This is an interesting finding as the sample received a visual ranking of five after only five cycles. This means that much of the top surface of the sample had been lost and there was still a large increase in the mass. The large mass gain from the solution is likely caused by a significantly different permeability of the 70% fly ash samples compared to the others at the time of the test. This higher permeability could allow the concrete to become critically saturated faster and hence decrease the salt scaling performance of the concrete. This will be investigated in future work.

As shown in Table 6, all of the mortar samples prepared from the same mixture as the concrete showed a lower visual ranking, lower mass loss, and lower rate of deterioration except the 70% fly ash samples which showed very similar performance between mortar and concrete. Since the concrete and mortar were taken from the same mixture, the only difference between these samples is the coarse aggregates. This suggests that the coarse aggregate plays an important role in the salt scaling performance of concrete. Including coarse aggregates in the mixture may cause larger transition zones. The transition zone is the boundary between the paste and the aggregate and is known to be weaker and more porous then the other areas in the paste. These larger transition zones may lead to weak areas that increase the susceptibility of the material to salt scaling. This finding will be investigated in future work.

Radiographs and Tomographs

The radiographs and tomographs provided a novel and useful way to look at the performance of the investigated mortars at the micron length scale. This testing has the potential to give great insight into the mechanisms. In almost every sample investigated there were some localized failures that were observed. One must realize that the entire sample is about 3/16" deep. This means that the sample would have to lose about 50% of the depth before the result would be significant in the ASTM C672 test. Also, these tests look at localized areas that may perform differently because of imperfections not regularly found in the bulk of the sample.

Despite all samples showing some deterioration, the samples that showed severe scaling in the ASTM C672 tests also showed severe scaling in the small scale tests. The sample that was not air entrained and the one that was air entrained with 70% fly ash showed significant deterioration as shown in Figures 2 and 10. The sample with no air entrainment (Figure 2) almost entirely disintegrated during the test. As the sample failed, there was almost no cracking observed in the sample, and large pieces were lost. The paste also seems to be preferentially lost around the fine aggregates. For the sample with 70% fly ash (Figure 10), large cracks in the paste that are parallel to the surface of the sample are observed after about 20 cycles. Material in the upper right hand of the sample is observed to be lost after 36 cycles. This sample was also used for investigation with the tomography in Figures 12, 13, and 14. The data shows that the largest amount of material was lost between zero to 16 cycles and 32 to 40 cycles. Figure 14 is also useful to show how the material was lost in layers parallel to the surface. Future work will be done to segment the data to show the difference between the aggregate and the paste in the samples. This will allow more insight to be provided.

It was also found that the 5/16" diameter samples showed a greater amount of damage from salt scaling then the samples with 3/16" diameter. The radiographs seem to suggest that as the number of fine aggregates increased in the samples then so did the rate of failure. This can be seen by closely looking at the results for Figures 2, 5, 7, 10, and 11. In all cases, the section loss occurs right above fine aggregate in the sample. The larger diameter samples will have a higher probability of including sand grains, so this may explain the increased rate of failure. This finding also agrees with the previous work done on the salt scaling tests that showed the mixtures with coarse aggregate showed a higher rate and amount of damage from salt scaling over those that just contained mortar. Both findings suggest that the transition zone is important in the failure process. In future work the research team will identify the location of the fine aggregates in the samples and correlate them with the location of damage. The precursor work to this is shown with the tomography data.

Conclusions

Some useful observations were made in this work. These include:

- Concrete samples that were air entrained with a 50% fly ash replacement showed satisfactory salt scaling performance despite the replacement value being larger than what is suggested in most specifications and building codes.
- When the fly ash replacement level was increased to 70% satisfactory salt scaling performance was not observed.
- When the coarse aggregate was removed from a mixture the resulting mortar showed improved performance in the salt scaling tests.
- The results from the samples investigated with mCT showed general agreement with the concrete tests.
- As the number of fine aggregates increased in the sample, it appears that the rate of deterioration from salt scaling also increased. This likely explains why the 5/16" diameter samples failed at a faster rate than the 3/16" samples.

While each of these observations is useful, more work is needed to further understand the salt scaling deterioration mechanisms. With additional work the 3D tomography data has great potential to provide powerful insights into the failure of concrete from salt scaling. The ability to quantitatively describe the geometry change of the paste, aggregates, and air voids at a micron length scale is quite useful to help better elucidate the performance, and the research in this area should continue to be supported.

REFERENCES

1. ASTM C150, 2011, "Standard Specification for Portland Cement," American Society for Testing and Materials, West Conshohocken, Pennsylvania.
2. ASTM C618, 2012, "Standard Specification for Coal Fly Ash and Raw or Calcined Natural Pozzolan for Use in Concrete," American Society for Testing and Materials, West Conshohocken, Pennsylvania.
3. ASTM C143, 2003, "Standard Test Method for Slump of Hydraulic Cement Concrete," American Society for Testing and Materials, West Conshohocken, Pennsylvania.
4. ASTM C672, 2012, "Standard Test Method for Scaling Resistance of Concrete Surfaces Exposed to Deicing Chemicals," American Society for Testing and Materials, West Conshohocken, Pennsylvania.
5. Whiting, D., "Deicer Scaling and Resistance of Lean Concretes Containing Fly Ash," fly Ash, Silica Fume, Slag, and Natural Pozzolans in Concrete, SP-114, American Concrete Institute, Farmington Hills, MI, 1989, pp. 349-372.

Part II: Durability Properties of High Volume Fly Ash Concrete

Final Report: May 2014

Jonathan Drury
Corey Wirkman
Jeffery Volz, Ph.D., S.E., P.E.

University of Oklahoma
School of Civil Engineering and Environmental Science
334 Carson Engineering Center
Norman, OK 73019

Introduction

Concrete is the world's most consumed man-made material. Unfortunately, the production of portland cement, the active ingredient in concrete, generates a significant amount of carbon dioxide. For each pound of cement produced, approximately one pound of carbon dioxide is released into the atmosphere. With cement production reaching nearly 6 billion tons per year worldwide, the sustainability of concrete is a very real concern.

Since the 1930's, fly ash – a pozzolanic material – has been used as a partial replacement of portland cement in concrete to improve the material's strength and durability, while also limiting the amount of early heat generation. From an environmental perspective, replacing cement with fly ash reduces concrete's overall carbon footprint and diverts an industrial by-product from the solid waste stream (currently, about 40 percent of fly ash is reclaimed for beneficial reuse and 60 percent is disposed of in landfills).

Traditional specifications limit the amount of fly ash to 25 or 30 percent cement replacement. Recent studies, including those by the investigators, have shown that higher cement replacement percentages – even up to 75 percent – can result in excellent concrete in terms of both strength and durability. Referred to as high-volume fly ash (HVFA) concrete, this material offers a viable alternative to traditional Portland cement concrete and is significantly more sustainable. By nearly doubling the use of reclaimed fly ash in concrete, HVFA concrete aligns well green initiatives on recycling.

However, HVFA concrete is not without its problems. At all replacement rates, fly ash generally slows down the setting time and hardening rates of concrete at early ages, especially under cold weather conditions, and when less reactive fly ashes are used. Furthermore, with industrial by-products, some variability in physical and chemical characteristics will normally occur, not only between power plants but also within the same plant. Consequently, to achieve the benefits of HVFA concrete, guidelines are needed for its proper application in bridges, roadways, culverts, retaining walls, and other transportation-related infrastructure components.

The objective of this research was to design, test, and evaluate the durability of HVFA concrete mixtures.

Experimental Methods

Materials

A Type I cement meeting the requirements of ASTM C150 and Type C fly ash according to ASTM C618 was used in this study. Table 1 shows the oxide analysis from X-ray Fluorescence (XRF). Locally available crushed limestone with a nominal maximum aggregate size of 3/4" was used as course aggregate and natural sand as the fine aggregate.

Table 1 – Oxide analysis of cement and fly ash.

Oxide	Chemical Test Results (%)	
	Cement	Fly Ash
SiO_2	20.40	33.46
Al_2O_3	4.41	19.53
MgO	2.11	5.54
Fe_2O_3	3.62	6.28
CaO	63.83	26.28
SO_3	2.49	2.40
Na_2O	0.20	1.73
K_2O	0.45	0.45
TiO_2	0.13	1.48
P_2O_5	0.16	1.30
SrO	0.20	0.40
BaO	0.03	0.84
MnO_2	-	0.03

Mixture Design

In this study, four concrete mixtures were used with water to cementitious material ratio (w/cm) of 0.45. One mixture used only Portland cement as the binder, which represented the control, while the HVFA concretes used 70% fly ash mass replacement of cement. Two HVFA concrete mixtures were studied with no air entraining agent (AEA), one with a relatively high total cementitious material content (730 lb/yd^3) and the other with a relatively low total cementitious material content (564 lb/yd^3). The final HVFA concrete mixture used AEA to achieve approximately 6% air content using the relatively low total cementitious material content. The mix designs are shown in Table 2.

Mixing Procedure

Aggregates were collected from outside storage piles and brought into the mixing room where they were thoroughly mixed and samples were taken for moisture correction. These samples were oven dried to obtain the moisture content of aggregates and the weights of each material was adjusted based on moisture condition. At the time of mixing, all aggregates were loaded into the mixer along with approximately one-third of the mixing water. This combination was mixed for three minutes to ensure that the aggregates were evenly distributed. Next, the cementitious materials and the remaining water were added and mixed for three minutes. The resulting mixture rested for two minutes while the sides of the mixing drum were scraped. After the rest period, the mixer was turned on and AEA was added (if applicable). After the addition of AEA the concrete was mixed for three minutes.

Table 2 – SSD Mixture Proportions used in this study.

Mixture Designation	Description	Cement (lb/yd^3)	Fly Ash (lb/yd^3)	Coarse Aggregate (lb/yd^3)	Fine Aggregate (lb/yd^3)	Water (lb/yd^3)	w/c
Control	100% Portland Cement	564	0	1860	1240	226	0.40
HVFA 1	High Cementitious Content	220	510	1750	1085	292	0.40
HVFA 2	Low Cementitious Content	170	395	1820	1240	226	0.40
HVFA 2A	HVFA 2 with 6% air	170	395	1860	1240	226	0.40

Fresh and Hardened Concrete Property Testing

Standard fresh and hardened property testing was completed on each of the four mixes. Fresh properties included slump (ASTM C143), air content (ASTM C138), and unit weight (ASTM C138). Hardened properties included compressive strength (ASTM C39) and modulus of elasticity (ASTM C469).

Rapid Freezing and Thawing

The test involves subjecting specimens to multiple freeze-thaw cycles in order to measure the resistance of the material to deterioration caused by the expansion of the free water freezing inside the specimens. This resistance was measured using three parameters: the length change of the specimens, change in the fundamental transverse frequency of the specimens, and mass change of the specimens. A decrease in the values for these parameters indicates freeze-thaw deterioration.

The specimens for the rapid freeze-thaw test were fabricated according to ASTM C 666–03, “Standard Test Method for Resistance of Concrete to Rapid Freezing and Thawing.” The molds used in the fabrication of these specimens are shown in Figure 1. These stainless steel molds measured 3.5 in. in width, 4.5 in. in height, and 16 in. in length and conformed to ASTM C 666 requirements for specimen dimensions.

Figure 1 – Freezing and Thawing Specimen Molds

The ends of each mold contained a threaded hole to install a specialized bolt. This bolt contained a rounded end, and when the concrete specimens were de-molded, the end of this bolt protruded from both ends of the prism. The embedded bolt provides a mechanism to measure the length change of the concrete prism as it was subjected to freezing and thawing cycles.

All specimens were tested in accordance with ASTM C 666, Procedure A. When the specimens reached the appropriate age, they were brought to the target thaw temperature. The fundamental transverse frequency, mass, length, and cross section of the specimen was measured. The freeze-thaw specimens were then subjected to the appropriate freezing and thawing cycles. Each specimen was subject to 300 cycles of freezing and thawing while submerged in water. Every 36 cycles the specimens would be removed at the thawed state and properties of the specimen would be measured. The properties measured were fundamental transverse frequency, length change, and mass change. The specimens were then placed back into the testing apparatus and the cycles continued. The test could be ceased if the specimen deteriorated so extensively that the test could not continue.

Rapid Chloride Ion Penetration

Chloride penetration of concrete is one of the leading durability issues facing many concrete specimens. Concrete members that are exposed to chlorides such as concrete piers in the ocean or concrete bridge decks exposed to de-icing salts all face chloride penetration. If sufficient chloride is allowed to penetrate into a concrete member, it can cause the embedded steel reinforcement to corrode and the expanding corrosion product will results in internal stresses, which in turn will cause cracking of the concrete. Over time this will cause concrete spalling and eventual failure. The electrical indication of concrete's ability to resist chloride penetration is a rapid method to determine the permeability of the concrete and its ability to withstand chloride penetration.

The test specimens consisted of cylinders fabricated and prepared according to ASTM C 192–07, "Standard Practice for Making and Curing Concrete Test Specimens in the Laboratory." Two 4 in.

diameter x 8 in. long cylinders were used for this test for every concrete mix. These cylinders were prepared alongside the compressive strength specimens. These specimens were de-molded after 24 hours and placed in the moist curing chamber for 28 days.

The rapid chloride ion penetration test is outlined in ASTM C 1202-10, “Standard Test Method for Electrical Indication of Concrete’s Ability to Resist Chloride Ion Penetration.” The test specimens consist of 4 in. diameter by 2 in. thick concrete disks. These disks were cut from specimens cast according to ASTM C 192. Two disks were cut from each concrete cylinder, with two concrete cylinders cast from each mix, which resulted in a total of 4 concrete disks for each concrete mix. One disk was cut from the top of the cylinder and the other from the middle. These disks were labeled with the mix design name and noted as either middle or top. The specimens were allowed to surface dry for at least 1 hour before the sides of the disks were coated with a setting coating as shown in Figure 2.

Figure 2 – Application of Setting Coating

After the coating dried, the specimens were placed into a vacuum desiccator and vacuumed for 3 hours. The pressure of the vacuum was at least 0.96 psi. At the end of the 3 hour desiccation period, de-aerated water was poured into the water stockpot of the vacuum until the specimen was covered. The stockpot was closed and the vacuum was maintained for another hour. The vacuum was then turned off and air was allowed to enter the desiccator. The specimen was then allowed to soak in the de-aerated water for 18 ± 2 hours. The specimen is then blotted dry and placed into the voltage cell. A sealant is then applied to the specimen-cell boundary. The exposed face of the specimen is then covered while the sealant is allowed to dry. Once the sealant is dry, the process is repeated to the other face of the specimen. The final specimen is shown in Figure 3.

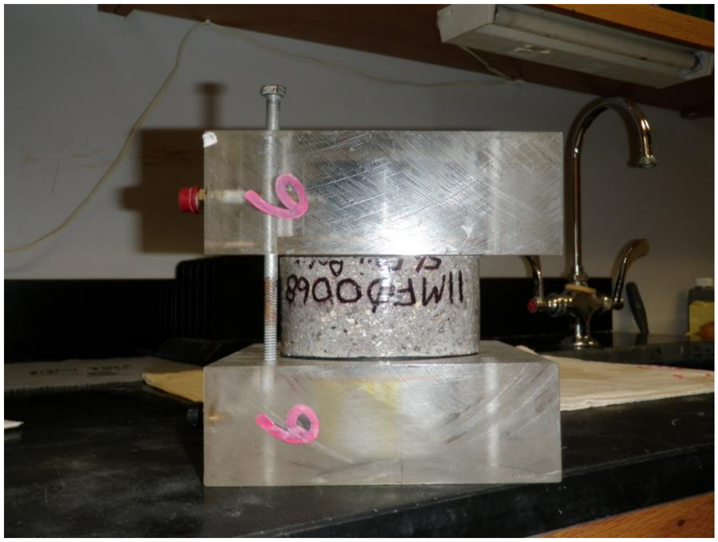

Figure 3 – Completed Rapid Chloride Specimen

The test setup is shown in Figure 4. The side of the cell that is connected to the negative terminal is then filled with 3.0% NaCI solution while the side connected to the positive terminal is filled with 0.3 N NaOH solution. The voltage is set to 60V and the initial current is recorded and then recorded at 30 minute intervals. The test is conducted for 6 hours. The data that is recorded is then used to calculate the total charge passed through the specimen in coulombs.

Figure 4 – Rapid Chloride Ion Test Setup

Ponding

A serious problem facing concrete bridge decks is spalling and deterioration caused by chloride penetration and subsequent corrosion of the underlying steel. During winter months, de-icing salts are used to remove snow and ice from bridge and roadway surfaces. The chlorides contained in these de-icing salts diffuse into the concrete, eventually breaking down the passive layer of the reinforcing steel and causing corrosion. The corrosion product expands to approximately six times the original volume, resulting in internal stresses and eventually cracking. Over time, this process will lead to spalling and deterioration of the concrete. The ponding test subjects concrete specimens to a similar environment to investigate the ability of the concrete to resist chloride penetration. This test is a valuable indicator of the resistance of the concrete to chloride ingress and thus the durability of the material. Although this test requires a longer period of time compared to other methods to predict the resistance of concrete to chloride penetration, it is the most realistic test method.

The concrete specimens for the ponding test were fabricated according to ASTM C 1543-10, "Standard Test Method for Determining the Penetration of Chloride Ion into Concrete by Ponding." Three specimens were made for each concrete mix. The test requires that the specimens have a surface area of at least 45.6 in^2. The specimens must also be at least 3.54 ± 0.6 in. tall. The specimens created for the ponding test in this investigation measured 18 in. wide x 18 in. long x 4 in. tall. Also, the test procedure required a dike along the top of the specimen with a height of at least 0.79 in. high. To accomplish this, a 0.75 in.-thick foam panel measuring 16 in. x 16 in. in plan was placed on a sheet of plywood that would serve as the base of the mold. Walls constructed from 2 in. x 4 in. pieces of wood were then connected to the panel to arrive at the overall dimension of 18 in. x 18 in. in plan. When the concrete was placed in the mold, the foam created a void in what would become the top of the specimen. The foam formed the reservoir for the chloride solution. The concrete was placed into the formwork and consolidated as necessary. After 24 hours, the concrete specimens were de-molded and placed in a moist curing chamber. After 14 days of moist curing, the specimens were transported to a temperature and humidity controlled environment where they would dry cure for another 14 days. After 28 days of curing, the specimens would then begin the ponding test.

The test procedure involved placing a 5% by weight chloride solution into the ponding specimen reservoir. The solution had to be at a depth of 0.6 ± 0.2 in. A photograph of a typical ponding specimen is shown in Figure 5. When the required amount of solution was poured into the reservoir, the concrete specimens were covered with plastic sheeting and the sheets were secured with elastic bands to prevent evaporation of the solution. Every two weeks, the specimens were checked to ensure that the proper depth of the solution was maintained. If the reservoir was low, additional solution was added. After 60 days of ponding, the reservoir was vacuumed dry and fresh solution was added. The sheeting was replaced and the specimens were monitored every two weeks. After another 60 days, the chloride solution was vacuumed off and the specimen allowed to air dry. A few days later, a core was taken from the center of the specimen to determine the chloride profile.

Figure 5 – Ponding Test Specimen

Salt Scaling

When concrete is exposed to freezing and thawing temperatures and is subjected to de-icing salts, it can deteriorate in the form of scaling. Scaling is defined as a general loss of surface mortar or mortar surrounding the coarse aggregate particles on a concrete surface. This occurs most often on bridge decks and roadways in cold climates. Scaling deterioration reduces the appearance, smoothness, and, most importantly, resistance of the concrete to further degradation.

The specimens used for the scaling test were fabricated as specified by ASTM C 672–03, "Standard Test Method for Scaling Resistance of Concrete Surfaces Exposed to Deicing Chemicals." These specimens are required to be at least 75 in^2 in plan and at least 3 in. in depth. The specimen form is shown in Figure 6. Three specimens were constructed for each concrete mix. The molds were formed from two steel channels connected by a steel pin. A plate was placed at the bottom of the channels.

The concrete was placed in the form in one lift and rodded 72 times. The concrete was placed with approximately one inch of the form remaining exposed. Once the concrete was placed into the mold and allowed to reach a firm state, the specimens were broom finished with a medium broom. Then, using the exposed 1 in. of form, a dike was constructed along the edges of the specimen. The dike was constructed using a mortar mix consisting of 3 parts fine aggregate, 2 parts Portland cement, and 1 part water. The dike was constructed by hand using putty knifes for forming. A 1 in. guide line was pressed into the edge of the fresh concrete to indicate the boundary of the dike. Keyways were then placed into the concrete where the dike would be constructed. The mortar was then placed onto the specimen and the dike was formed. A completed specimen is shown in Figure 7.

The testing procedure consisted of subjecting the specimen to freezing and thawing cycles in the presence of a saltwater solution within the reservoir formed by the dikes. A chloride solution measuring approximately 0.25 in. deep was placed into the reservoir of the specimen. The specimen was then placed into a walk-in freezer where it remained for 16 to 18 hours at a temperature of 32°F. After that period of time, the specimen was removed from the freezer and placed in a temperature and humidity-controlled environment of 73.5± 3.5°F and 45 to 55% R.H. for a period of 6 to 8 hours. This sequence counted as one cycle. Chloride solution was periodically added as necessary to maintain the proper depth, and the solution was completely replaced every 5 cycles. After 50 cycles the surface of the specimens was inspected and the degree of scaling was reported based on the ASTM standard.

Figure 6 – Scaling Specimen Form

Figure 7 – Salt Scaling Specimen

Results

Fresh and Hardened Concrete Properties

Slump, air content, unit weight, compressive strength, and modulus of elasticity are reported for each mixture in Table 3. Compressive strength and modulus of elasticity were measured after 28 days of moist curing, with the values shown in Table 3 representing the average of three specimens.

Table 3 – Fresh and hardened concrete properties.

Mixture	Slump (in.)	Air Content (%)	Unit Weight (pcf)	28-Day Compressive Strength (psi)	Modulus of Elasticity (ksi)
Control	4.5	1.3	149	5,370	4,067
HVFA 1	7.0	1.1	144	4,120	3,554
HVFA 2	5.5	1.5	146	3,410	3,118
HVFA 2A	6.0	1.4	146	3,285	3,121

As expected, the compressive strength decreased with the high amounts of fly ash. This result was somewhat mitigated by the HVFA concrete mix with the relatively high total cementitious content (HVFA 1). Also, because of the increased slump due to the fly ash, it is possible to reduce the water content of these mixes to further mitigate the loss of compressive strength.

Rapid Freezing and Thawing

The dynamic modulus of elasticity was recorded at several intervals, though not to exceed 36 cycles of freeze-thaw throughout the testing. An oscillator with ranging values of frequencies was used to find the lowest frequency at which each specimen would resonate. A conversion equation was then used to convert the fundamental transverse frequency to dynamic modulus of elasticity. This procedure was repeated until each specimen had undergone 300 freeze-thaw cycles.

The results from the freeze-thaw testing are shown in Table 4. A reported durability factor greater than 80 percent classifies a concrete mix as having “good” freeze-thaw resistance. Only one mix design, the air entrained HVFA concrete mix exceeded the 80 percent threshold for a good rating. The HVFA 2 mix performed comparably to the control mix design, and the improved performance of mix HVFA 2A is thus directly attributable to the air entrainment. This result indicates that, in general, high amounts of fly ash do not reduce the freeze-thaw resistance of concrete. However, HVFA 1, the high total cementitious content mixed showed slightly poorer performance than the control. This results may be attributable to the more tortuous pore structure resulting from the higher amount of fly ash. This pore structure, without the addition of air entrainment, does not allow for easy expansion of the free water, reducing the freeze-thaw performance.

Table 4 – Freeze-Thaw Durability Results.

Mixture	Specimen	Durability Factor (%)	Average Durability Factor (%)
Control	C-FT1	77.3	75.6
	C-FT2	74.5	
	C-FT3	75.0	
HVFA 1	HVFA 1-FT1	68.1	69.3
	HVFA 1-FT2	72.1	
	HVFA 1-FT3	67.6	
HVFA 2	HVFA 2-FT1	79.7	76.4
	HVFA 2-FT2	74.5	
	HVFA 2-FT3	75.1	
HVFA 2A	HVFA 2A-FT1	81.7	82.9
	HVFA 2A-FT2	84.3	
	HVFA 2A-FT3	82.6	

Rapid Chloride Ion Penetration

The testing and calculations for this test were performed in accordance with ASTM C 1202-10. After the testing was complete, the measured current vs. time was plotted. A trend line was drawn through the graph and was integrated to calculate the area under the curve. This area gives the total charge in coulombs to pass through the specimen during the 6 hour test. The total charge was then compared to Table 4.1 in ASTM C 1202 to assign a permeability rating, with a range from negligible (indicating the highest resistance to chloride penetration) to high (indicating the lowest resistance to chloride penetration). The ranges for the classes are as follows: 0-100 for negligible, 100-1000 for very low, 1000-2000 for low, 2000-4000 for moderate, >4000 for high. The results for the four mixes, control plus three HVFA concrete mixes, are shown in Table 5.

The results indicate that the HVFA concrete mixes performed better than the control mix. The control mix had a moderate permeability rating, while the two low total cementitious content HVFA concrete mixes (HVFA 2 and HVFA 2A) had low permeability ratings with the high total cementitiuos content HVFA concrete mix (HVFA 1) having the best permeability rating, that of very low. However, all three HVFA concrete mixes performed very close to each other, with average charge passed of 861, 1122, and 1030 for HVFA 1, HVFA 2, and HVFA 2A, respectively.

Table 5 – Rapid Chloride Ion Penetration Results.

Mixture	Specimen	Charge Passed (Coulombs)	Average Charge Passed	Permeability Class
Control	C-1 Top	2070	2008	Moderate
	C-1 Middle	1988		
	C-2 Top	2010		
	C-2 Middle	1964		
HVFA 1	H1-1 Top	876	861	Very Low
	H1-1 Middle	890		
	H1-2 Top	883		
	H1-2 Middle	796		
HVFA 2	H2-1 Top	1101	1122	Low
	H2-1 Middle	1009		
	H2-2 Top	1222		
	H2-2 Middle	1156		
HVFA 2A	H2A-1 Top	1093	1030	Low
	H2A-1 Middle	1001		
	H2A-2 Top	1027		
	H2A-2 Middle	999		

Ponding

The results for the chloride ponding tests are shown in Figure 8. The results are consistent with the rapid chloride permeability tests discussed previously. In general, HVFA concrete mix HVFA 1 showed the least ingress of chlorides throughout the specimen depth, while the control mix showed the greatest amount of chlorides, with HVFA 2 and HVFA 2A falling between the two although closer to the HVFA 1 mix. It is important to note that the ponding test is a relative measure of durability.

Salt Scaling

The scaling resistance test was performed in accordance with ASTM C 672-03. After being subjected to 50 freezing and thawing cycles while being ponded with chloride solution, the surface of the specimens were inspected and the appearance assigned a number depending on deterioration. The rating scale is provided in Table 6. The results for each mix are shown in Table 7. As indicated by the ratings, the three HVFA concrete mixes performed very poorly. In fact, the specimens reached the poorest scaling rating at around 30 cycles, well before completion of the full test.

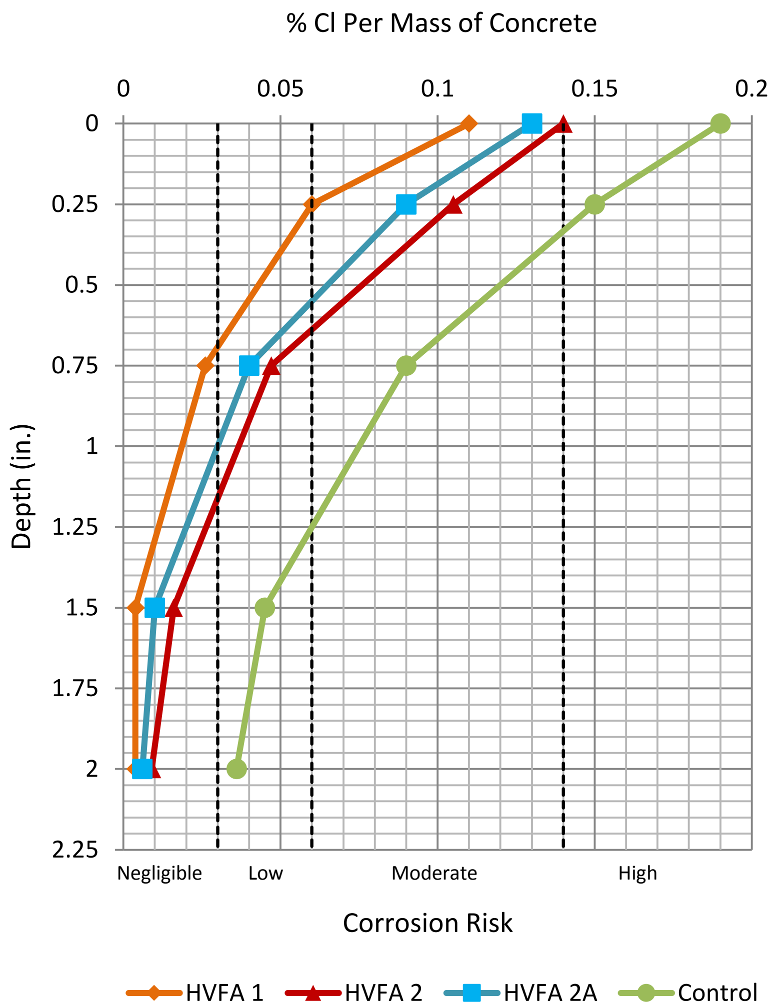

Figure 8 – Chloride Profiles

Table 6 – Salt Scaling Rating Scale.

Rating	Condition of Surface
1	No Scaling
2	Very Slight Scaling
3	Slight to Moderate Scaling
4	Moderate Scaling
5	Moderate to Severe Scaling

Table 7 – Salt Scaling Results.

Mixture	Specimen	Durability Factor (%)
Control	C-SC1	3
	C-SC2	3
	C-SC3	4
HVFA 1	HVFA 1-SC1	5
	HVFA 1-SC2	5
	HVFA 1-SC3	5
HVFA 2	HVFA 2-SC1	5
	HVFA 2-SC2	5
	HVFA 2-SC3	5
HVFA 2A	HVFA 2A-SC1	5
	HVFA 2A-SC2	4
	HVFA 2A-SC3	5

Discussion

In general, the HVFA concrete mixes performed very well with regard to common durability requirements. The HVFA concrete mixes outperformed the control mix in terms of freeze-thaw resistance and chloride permeability, both rapid and ponding tests. However, the HVFA concrete mixes performed very poorly with regard to salt scaling, reaching the worst rating prior to completion of the full number of cycles.

REFERENCES

1. ASTM C150, 2011, "Standard Specification for Portland Cement," American Society for Testing and Materials, West Conshohocken, Pennsylvania.
2. ASTM C618, 2012, "Standard Specification for Coal Fly Ash and Raw or Calcined Natural Pozzolan for Use in Concrete," American Society for Testing and Materials, West Conshohocken, Pennsylvania.
3. ASTM C143, 2003, "Standard Test Method for Slump of Hydraulic Cement Concrete," American Society for Testing and Materials, West Conshohocken, Pennsylvania.
4. ASTM C672, 2012, "Standard Test Method for Scaling Resistance of Concrete Surfaces Exposed to Deicing Chemicals," American Society for Testing and Materials, West Conshohocken, Pennsylvania.